Fragmentation patterns of multicharged C_{60}^{r+} ($r=3-5$) studied with well-controlled internal excitation energy

S. Martin,[1] L. Chen,[1,*] A. Salmoun,[2] B. Li,[1] J. Bernard,[1] and R. Brédy[1]

[1]*Université Lyon 1, CNRS, LASIM UMR 5579, 43 Boulevard du 11 Novembre 1918, F-69622 Villeurbanne, France*

[2]*Laboratory of Instrumentation Measure and Control, Physics Department Faculty of sciences, University Chouaïb Doukkali, B.P. 20 El Jadida, Morocco*

(Received 20 December 2007; published 4 April 2008)

We have studied the relaxation of triply charged C_{60} obtained in collisions $F^{2+}+C_{60}\rightarrow F^{-}+C_{60}^{3+*}$ at low impact energy ($E=6.8$ keV). Depending on the excitation energy, these initial parent ions decay following a variety of channels, such as thermal electronic ionization, evaporation of C_2 units, asymmetrical fission, and multifragmentation. Using a recently developed experimental method, named collision-induced dissociation under energy control, we were able to measure the energy deposited in C_{60}^{3+*} for each collision event and to obtain an excitation energy profile of the parent ions associated with each decay channel. In our chosen observation time scale of the order of 1 μs, evaporations and asymmetrical fissions of $C_{60}^{3+,4+}$ occur when the internal energy is in the range from 40 to 100 eV. The multifragmentation becomes dominant for multicharged $C_{60}^{4+,5+}$ parent ions from 100 to 210 eV. In the case of C_{60}^{4+}, the multifragmentation channel is opened at low energy (40 eV). Therefore, in the energy range 40–100 eV, the asymmetrical fission, evaporation, and multifragmentation channels are in competition.

DOI: 10.1103/PhysRevA.77.043201 PACS number(s): 36.40.Qv, 34.50.Gb, 34.70.+e

I. INTRODUCTION

The fragmentation of C_{60} has drawn great attention from a broad range of scientific communities during the last decade. A large number of experimental and theoretical studies have been dedicated to C_{60} using single-photon or multiphoton excitation [1–3], electron impact [4–6], and collisions with neutral or charged atoms [7–12]. The specific scientific interest in the C_{60} molecule, considered now as a model system, is related to its exceptional symmetric and stable structure. It offers the opportunity to prepare easily a mass-selected neutral cluster jet in the laboratory. The fragmentation of C_{60} depends sensitively on its charge and internal excitation energy. Generally speaking, hot multicharged C_{60} fullerenes decay by the multifragmentation (MF) process. In collisions between multicharged ions and C_{60}, multicharged C_{60} with relatively low internal energy can be prepared via an electron exchange process. With this method, the asymmetric fission (AF) of C_{60} has been observed for a charge state as high as 9 [8].

In most fragmentation studies, information on the internal energy of C_{60} prior to fragmentation was obtained by measuring the appearance energy (AE) of the fragment. In general, the cross section of a specific dissociation channel characterized by a daughter ion—for example, C_{58}^{+} resulting from the evaporation of a C_2 unit—was measured as a function of the kinetic energy of the incident particles (electrons, atoms, or ions) or the energy of the photons [3]. At the AE, the effective energy conversion efficiency (ECE) from the incident particle to the target was assumed to be about 100%. Beyond the AE, the ECE decreases due to the increasing part of the kinetic energy carried out by the scattered particle or by the ejected electrons. In these cases, a complete energy analysis of all particles involved in a single interaction should be required to evaluate the energy deposited in the target by the energy conservation relation.

So-called double-charge-transfer spectroscopy (DCTS) has been developed to measure the second ionization potential of diatomic molecules [13–16]. Recently, we have extended this method to study the fragmentation of C_{60} [17]. This extended method is named, thereafter, collision-induced dissociation under energy control (CIDEC). In a CIDEC experiment, the kinetic energy of the incident ion beam is kept constant. The energy deposited in the target is "scanned" due to the random distribution of the impact parameter. Events corresponding to grazing collisions where the scattered projectile carries a negative charge are selected. For such collision channels, a simple relation between the energy deposited E_d on the target, the energy defect δ of the reaction, and the kinetic energy loss ΔE of the projectile can be established easily, $E_d=\Delta E-\delta$ (see Ref. [17]). The key point of this method is based on the well-known atomic energy level occupied directly by the transferred electrons. As the excited states of the anions involved in our experiments are unstable and generally lead to neutralization in a time scale shorter than 100 ns [14], we reasonably consider that the scattered atomic anions are prepared in the ground state. Therefore, by measuring the kinetic energy loss of the anion, it is possible to determine the energy deposited in the target during the collision and to measure the relative cross section of a specific dissociation channel versus the excitation energy of the parent C_{60}.

We have reported in a recent paper [18] the measurement of the cross sections of the evaporation channels of C_{60}^{2+*} prepared in the collision $H^{+}+C_{60}\rightarrow H^{-}+C_{60}^{2+*}$ with the CIDEC method. Narrow excitation energy windows corresponding to the detection of C_{58}^{2+}, C_{56}^{2+}, and C_{54}^{2+} were observed. These narrow peaks were in contrast with the typical broad shaped curves obtained in photon or electron im-

*chen@lasim.univ-lyon1.fr

pact measurements as a function of the energy of the incident particle. The measured distributions were simulated with a statistical-cascade model without any hypothesis on the internal energy distribution of the parent C_{60}.

In the present paper, we study the decay of C_{60}^{3+*} parent ions using the CIDEC method in the collision $F^{2+}+C_{60} \rightarrow F^{-}+C_{60}^{3+*}$. The main interests of this reaction are first to produce C_{60} ions at higher initial charge state and second to produce hotter C_{60} in order to study the decay in a larger internal excitation energy range. In such collisions, three time scales can be distinguished. During the collision, the electron capture and energy deposition via electronic interaction occur in a very short time scale, less than 1 fs. Then, competition between the thermal electronic ionization (TEI) and the energy transfer from the electronic to the vibronic degrees of freedom leading to the heating of the C_{60} cage takes place in a time range of ps. The TEI leads to a fast loss of electrons and the formation of intermediate parent ions at a higher charge state, C_{60}^{4+} or C_{60}^{5+}. Finally, the excited C_{60}^{3+*} or intermediate-parent ions C_{60}^{r+*} ($r=4,5$) decay via dissociation in a larger time scale.

In a previous experiment [17], the ratio for the production of F^- via three-electron capture was measured to be about 3% of the total charge exchange cross section and the energy deposited in the C_{60} to be from 40 to 200 eV. In the present work, we report on the excitation energy distribution of the parent ions for each fragmentation and ionization channel. The center and width of the measured energy windows associated with a large number of decay channels are presented. From these data, it is possible to get more insight into the decay dynamics of the C_{60} via evaporation of C_2 units, thermoelectronic ionization, asymmetrical fission, and multifragmentation.

II. EXPERIMENT

The experimental setup used in this work has been described in detail elsewhere [8,17]. The projectile ions F^{2+} were extracted from the electron cyclotron resonance (ECR) Nanogan 3 source at Lyon at a voltage of 3000 V providing a typical ion current of about 1 nA in the interaction region. The crystalline fullerene powder (consisting of approximately 99% of C_{60} and 1% of C_{70}) was evaporated in an oven heated to 500 °C. The effusive beam formed by the C_{60} vapor crossed the F^{2+} ion beam at right angles between two extraction plates polarized to −350 V and −450 V, respectively. The collision energy was therefore 6.8 keV at the crossing point of the two beams where the electrostatic potential was −400 V. Electrons and recoil ions including stable C_{60}^{r+}, charged fullerenes, and smaller fragments were extracted by a transverse electric field of 100 V/cm. The energy loss of scattered negative fluorine ions was analyzed using a translational energy spectrometer (resolution of 400) composed of a cylindrical electrostatic analyzer (radius 205 mm) with an exit slit adjusted to 100 μm. The size of the incoming F^{2+} beam was drastically reduced using a small slit (width 100 μm, height 500 μm) placed just before the interaction region to improve the resolution.

The recoil ions accelerated to 2 keV were analyzed by a standard time-of-flight (TOF) tube of about 850 mm in length. They were post-accelerated with a voltage of 3.4 kV toward a detector equipped with two multichannel plates (MCP) and a multianode of 128 pixels linked with 128 individual discriminators. This device was particularly useful for detecting identical ions and for measuring precisely their multiplicities in the MF of highly charged C_{60} parent ions. The electrons ejected due to the fast TEI from the initial parent C_{60}^{3+*} were detected using a semiconductor detector that measured the number n of electrons. The charge r of the intermediate parent ion prior to the fragmentation was then determined with the electron number conservation rule $r=n+3$ (three electrons are stabilized on the projectile). To record a spectrum, the scattered F^- ions were selected according to their kinetic energy loss by scanning the voltage of the electrostatic analyzer. For each voltage, the TOF of recoil ions and the ejected electron number were measured in multicoincidence and in event-by-event data acquisition mode. During our experiments, the single-collision condition was satisfied.

III. EXPERIMENTAL RESULTS AND DISCUSSIONS

A. Triply charged fullerenes

A typical two-dimensional (2D) spectrum, named in the following the excitation-energy recoil-ion (EX-RI) spectrum [Fig. 1(a)], was built by plotting the recoil-ion TOF along the horizontal axis and the voltage of the projectile analyzer for detecting F^- anions along the vertical axis. The vertical scale should be converted first to the kinetic energy loss of F^- and then to the excitation energy of the target based on the CIDEC method. However, an absolute calibration of the electrostatic analyzer is not evident. In our previous experiment using singly charged projectiles in $F^{+}+C_{60} \rightarrow F^{-}+C_{60}^{2+*}$ reactions [17], the kinetic energy loss of the anion F^- was calibrated by means of collisions with rare-gas argon atoms. This method is not suitable in the present case, because the F^- production cross section in the collisions $F^{2+}+Ar \rightarrow F^{-}+Ar^{3+}$ is too small. However, in both collision experiments using F^+ and F^{2+} projectiles, C_{58}^{3+} fullerenes were obtained. In the first case, the C_{58}^{3+} fullerenes were obtained from the C_{60}^{2+*} primary ions via first TEI ($C_{60}^{2+*} \rightarrow C_{60}^{3+*}+e^{-}$) and second the evaporation of a C_2 unit from the intermediate parents C_{60}^{3+*} ($C_{60}^{3+*} \rightarrow C_{58}^{3+}+C_2$). Assuming that the kinetic energy of the TEI electron is negligible, the internal energy of the intermediate parent ion C_{60}^{3+*} that undergoes further evaporation of a C_2 was estimated by subtracting the third ionization energy of C_{60} from the measured excitation energy of the initial C_{60}^{2+*} parent ion. The obtained value 46.8 eV of the internal energy was used in the present experiment to assign the center of the C_{58}^{3+} peak, which allows us to calibrate directly the excitation energy of the target C_{60}^{3+}.

Projection of this EX-RI spectrum onto the horizontal axis leads to the TOF spectrum of the recoil ions shown in Fig. 1(b). In principle, from the partial projection onto the vertical axis of each spot in Fig. 1(a), one can extract the excitation energy distribution of the initial parent ions C_{60}^{3+*} related to each group of recoil-ion fragments with the same mass over charge ratio m/q, where m stands for the atomic mass of the

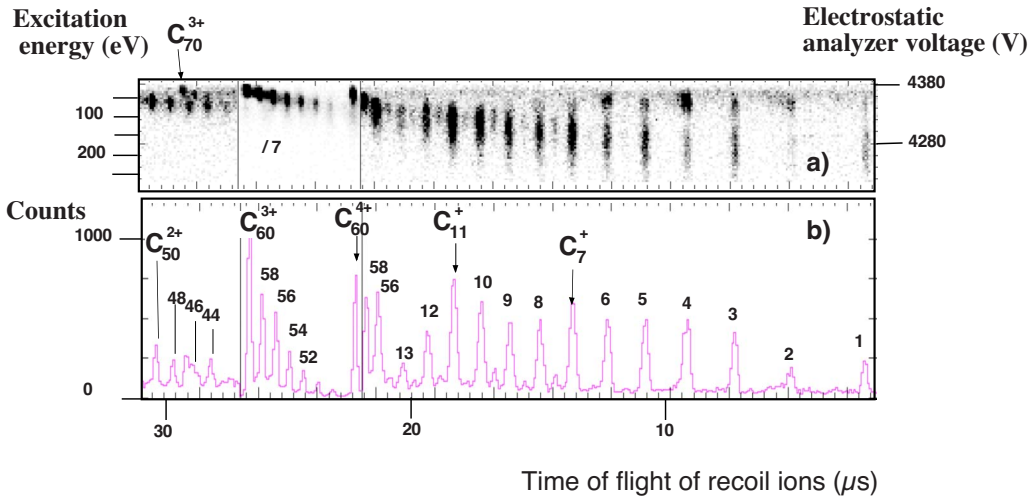

FIG. 1. (Color online) (a) EX-RI spectrum recorded in $F^{2+}+C_{60}\rightarrow F^{-}+C_{60}^{3+*}$ collisions. Horizontal axis: TOF of recoil ions. Vertical axis: right scale, electrostatic analyzer voltage; left scale, excitation energy of the initial C_{60}^{3+*} parent ions. (b) Projection of (a) onto the horizontal axis. The spots and the peaks between C_{60}^{3+} and C_{60}^{4+} in (a) and (b) are reduced by a factor of 7.

ion divided by 12. The spot at $m/q=20$ is attributed without ambiguity to C_{60}^{3+}. From the projection onto the vertical axis of this spot, we obtained a raw profile of the internal excitation energy of intact C_{60}^{3+} ions. This raw profile was fitted then with a Gaussian distribution convoluted by the instrumental broadening function of 7 eV in full width at half maximum (FWHM). The obtained Gaussian distribution, called the measured excitation energy distribution, is centered at $E_c=38.8$ eV (Table I) with a width (FWHM) of $\Delta=11.2$ eV (Table II). In the following, measured energy distributions associated to other fragmentation channels were obtained with the same data analysis method. Comparing to the doubly charged C_{60}^{2+} produced by two-electron capture [17,18], the C_{60}^{3+} ions are produced at a quite larger excitation energy. This is mainly due to the larger energy defect of the present reaction $\delta=-22.2$ eV. This value was calculated using the ionization potentials (IPs) and the electron affinity (EA) of fluorine ($IP_1=17.4$ eV, $IP_2=34.9$ eV, EA=3.4 eV) [14] and the IP(s) of C_{60} ($IP_1=7.8$ eV, $IP_2=11.3$ eV, $IP_3=14.4$ eV) [19].

A certain number of spots in Fig. 1(a) can be related to several decay-channels. The spots of triply charged fullerenes may result from either the evaporation of C_{60}^{3+*} or the AF of C_{60}^{4+*} and C_{60}^{5+*}. The contributions of intermediate parent ions $C_{60}^{(3+n)+*}$ resulting from the loss of n electrons due to the fast TEI process are differentiated by measuring the number n of ejected electrons. To measure precisely the excitation energy of the evaporation channels of the fragmentation-parents C_{60}^{3+*}, we build an EX-RI spectrum [Fig. 2(a)] exclusively for events in which two conditions were fulfilled. First, no electron was detected ($n=0$) to ensure that the charge of the parent ion before fragmentation was 3. Second, only one charged fragment was detected by the MCP per event. The residual small peak of C_{60}^{4+} in the spectrum [Fig. 2(a)] was due to the limited electron detection efficiency (83%). The restrictive condition on the number of

TABLE I. E_c: center of the measured excitation energy distributions of the initial parent ions C_{60}^{3+} undergoing directly the evaporation leading to C_{60-2m}^{3+} or first the fast TEI and then the evaporation or AF from the intermediate parent ions C_{60}^{4+} leading to C_{60-2m}^{4+} or C_{60-2m}^{3+}, respectively. Values are given in eV.

	Evaporation of C_2 unit		Fission of intermediate parent C_{60}^{4+} ions leading to two charged fragments measured in coincidence: C_n^+ ($n=2,3,4,6$) and C_{60-2m}^{3+} (first column)			
Number of C atoms in the fullerene fragment	from initial parent ions C_{60}^{3+}	from intermediate parent ions C_{60}^{4+}	C_2^+	C_3^+	C_4^+	C_6^+
50	71.3			98.8		87.3
52	65.5		87.7	90.4	86.6	75.9
54	60.3		81.1	75.7	73.6	
56	53.9	71.5	70		68.5	
58	46.8	64.4	63.4			
60	38.8	49.2				

TABLE II. Δ: width (FWHM) of the measured excitation energy distributions of the initial parent ions C_{60}^{3+} (as in Table I) undergoing direct evaporation or fast TEI followed by the evaporation or AF from the intermediate parent ions C_{60}^{4+}. Values are given in eV.

	Evaporation of C_2 unit		Fission of C_{60}^{4+} leading to two charged fragments measured in coincidence: C_n^+ (n=2,3,4,6) and C_{60-2m}^{3+} (first column)			
	from the initial parent ions	from the intermediate parent ions				
Number of C atoms in the fullerene fragment	C_{60}^{3+}	C_{60}^{4+}	C_2^+	C_3^+	C_4^+	C_6^+
50	14.7			17.5	14.0	15.3
52	15.4		15.4	12.7	18.4	12.8
54	14.5		20.1	13.6	14.2	
56	12.7	12.8	17.2		10.1	
58	11.4	12.9	11.7			
60	11.2	15.1				

detected fragments is necessary to reduce the contribution of the AF from C_{60}^{4+} in case the ejected electron was not detected. From the projection onto the vertical axis of each spot of this spectrum, we obtained the raw profiles of excitation energy of the parent C_{60}^{3+} ions for the evaporative sequence $C_{60}^{3+} \rightarrow C_{60-2m}^{3+} + mC_2$ (not shown in Fig. 2) and then the measured excitation energy distributions noted $N(C_{60-2m}^{3+}, E)$ after correction for instrumental broadening. The center E_c and the width Δ (FWHM) of the distributions $N(C_{60-2m}^{3+}, E)$ are presented in the Tables I and II, respectively. In Fig. 3, the value of E_c is plotted as a function of the fullerene fragment size. The linear dependence of E_c on the size is in agreement with the well-known C_{60} relaxation dynamics via sequential evaporation of C_2 units as shown in Ref. [5]. From the data in Table I and II, it is also possible to estimate the appearance energy for each evaporation channel. For instance, to produce C_{50}^{3+}, the energy distribution is centered at E_c=71.3 eV with a width of Δ=14.7 eV. It can be considered that the production of C_{50}^{3+} becomes possible at an "equivalent appearance energy" calculated using the simple relation E_c-Δ=56.6 eV. In an electron impact experiment [5] in which the observation time scale (1 μs) was very close to ours (1.3 μs), the appearance energy was measured to be 58.5 eV, very close to our value. Direct comparison with the results obtained by UV photon excitation [2,3] was more difficult due to the very different observation time scales (up to 100 μs) and different extraction methods. Nevertheless, the general tendencies for appearance energies agreed with our results.

The measured excitation energy distributions $N(C_{60-2m}^{3+}, E)$ are presented in Fig. 4 for the three main dissociation channels (m=1,2,3) corresponding to the first

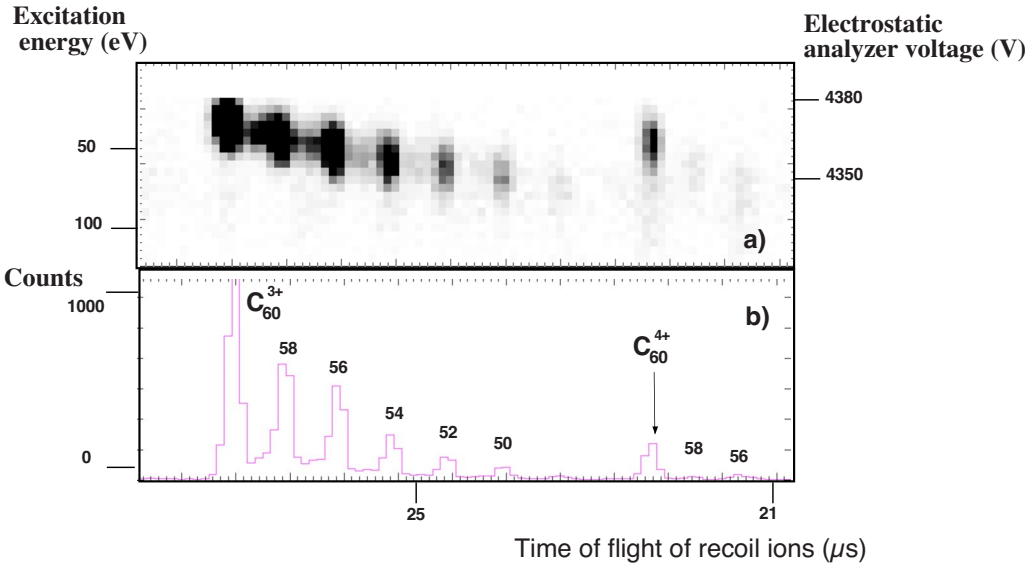

FIG. 2. (Color online) (a) EX-RI spectrum recorded in $F^{2+}+C_{60} \rightarrow F^- + C_{60}^{3+*}$ collisions with extra conditions to ensure that the parent of the fragmentation process is C_{60}^{3+}. (b) Projection of (a) onto the horizontal axis showing the evaporation sequence of C_{60}^{3+} fragmentation parent ions.

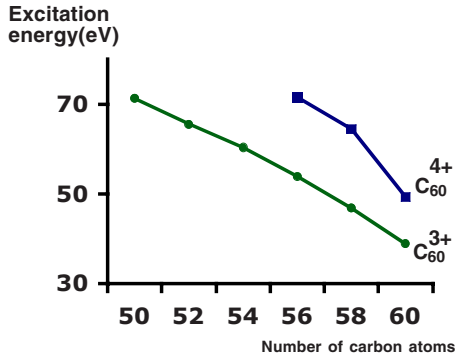

FIG. 3. (Color online) The center of the excitation energy profile for the evaporation channels leading to C_{60-2m}^{3+} and C_{60-2m}^{4+} fullerene ions from the fragmentation parents C_{60}^{3+} (circle) and C_{60}^{4+} (square).

steps of the evaporative sequence from C_{60}^{3+} ions leading to triply charged fullerenes C_{58}^{3+}, C_{56}^{3+}, and C_{54}^{3+}. These curves are simulated using a cascade model (see Ref. [18] for details) for the time window (1.3 μs) of this experiment. The decay rate for the evaporative cooling process was calculated with the Arrhenius formula based on the Rice-Ramsperger-Kassel (RRK) statistical model [20]. The preexponential factors were extracted from recent work [21], $A_{60}=1.2\times10^{21}$ s^{-1} and $A_{58,56,54}=2\times10^{19}$ s^{-1}. The dissociation energy, D^{3+} for each fullerene parent was adjusted as a free parameter in order to reproduce the experimental distributions. The best fit was obtained (Fig. 4) using the dissociation energies D_{60}^{3+}, D_{58}^{3+}, and D_{56}^{3+} presented in Table III. These values are comparable to the theoretical *ab initio* calculations of Ref. [22]. Therefore, our measured internal energy distributions are in good agreement with the one expected within the statistical evaporative cooling model. Nevertheless, an enhanced energy resolution is still required in order to test the theoretical models with a better precision.

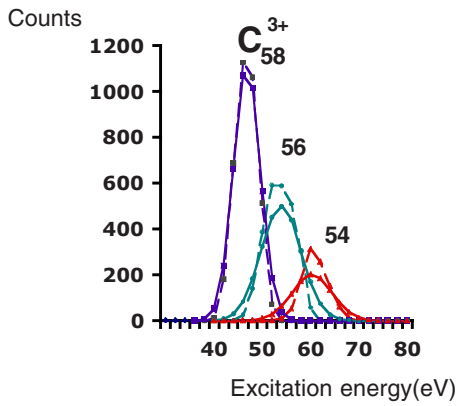

FIG. 4. (Color online) Symbols linked with solid lines: experimental population distributions of evaporation products, C_{58}^{3+}, C_{56}^{3+}, and C_{54}^{3+} fullerene fragments, as a function of the excitation energy of the parent ions C_{60}^{3+}. Symbols linked with dashed lines: theoretical modeling. The lines in this figure are to guide the eyes.

B. Quadruply charged intermediate parent ions: Evaporation

To study the decay of the intermediate parent ions C_{60}^{4+} resulting from the TEI ($C_{60}^{3+*}\rightarrow C_{60}^{4+*}+e^{-}$) of one electron, an EX-RI spectrum [Fig. 5(a)] has been extracted from the data files by selecting events in which one and only one electron was detected. The TOF spectrum [Fig. 5(b)] obtained by the projection of Fig. 5(a) onto the horizontal axis presents peaks attributed to quadruply charged fullerenes (C_{58}^{4+} and C_{56}^{4+}) resulting from evaporation processes, triply charged fullerenes (C_{58}^{3+}, C_{56}^{3+}, C_{54}^{3+}, C_{52}^{3+}, and C_{50}^{3+}) due to the AF processes, and small fragments (C_n^{+}, $n=1-15$) due to the MF processes.

In Fig. 5(a), the spots corresponding to C_{60}^{4+} and C_{56}^{4+} are slightly mixed respectively with the spots of C_{15}^{+} and C_{14}^{+}. However, an unambiguous attribution can be obtained by analyzing the number of charged fragments detected in a single event. From the data on Fig. 5(a) and by extracting events in which one and only one charged fragment was detected, another EX-RI spectrum (not showed here), only composed of spots of C_{60}^{4+}, C_{58}^{4+}, and C_{56}^{4+} ions, has been built. The center E_c and width Δ of the excitation energy distribution of the associated initial C_{60}^{3+*} parent ions are given in the Tables I and II, respectively. The excitation energy E_c is also displayed in the Fig. 3. Let us recall here that in the tables and figures of this paper, the measured excitation energies concern the initial parent ions C_{60}^{3+*} even for dissociation channels involving intermediate-parent ions of higher charge state. Comparing with the values obtained for triply charged fullerenes, an energy shift of about 17.2 eV is observed for the couples of fullerene products with the same size but different charge C_{58}^{4+}-C_{58}^{3+} and C_{56}^{4+}-C_{56}^{3+}, while the widths of the excitation energy distributions are very close for the above fullerene couples. In the case of C_{56}, for instance, the energy distributions of the parent C_{60}^{3+} ions related to the couple of evaporation channels, $C_{60}^{4+}\rightarrow C_{56}^{4+}+2C_2$ and $C_{60}^{3+}\rightarrow C_{56}^{3+}+2C_2$, have similar profiles. Assuming that the dissociation energy D for the evaporation of a C_2 unit depends only slightly on the charge of the parent ions, these two channels should be opened, respectively, for C_{60}^{3+} and the intermediate parent ions C_{60}^{4+} in the same internal energy window. The shift between the two profiles corresponds therefore to the energy necessary for producing the quadruply charged fullerenes C_{60}^{4+} from the initial C_{60}^{3+}. The measured value $E_c(C_{60-2m}^{4+})$-$E_c(C_{60-2m}^{3+})$ is close to the fourth ionization potential of C_{60}, $IP_4=17.8$ eV [19]. This result suggests that in the cases when the initial energy is shared between the fast TEI and the transfer to the vibronic degrees of freedom, the kinetic energy carried by the ejected electron is quasi-negligible. This is also in good agreement

TABLE III. Dissociation energy D_{60-2n}^{3+} ($n=0,1,2$) for the evaporation of a C_2 unit from a triply charged fullerene C_{60-2n}^{3+}. (a) this work and (b) Ref. [22].

(eV)	C_{60}	C_{58}	C_{56}
D^{3+} (a)	9.2 ± 0.9	8.2 ± 0.9	8.2 ± 0.9
D^{3+} (b)	9.9	8.9	8.7

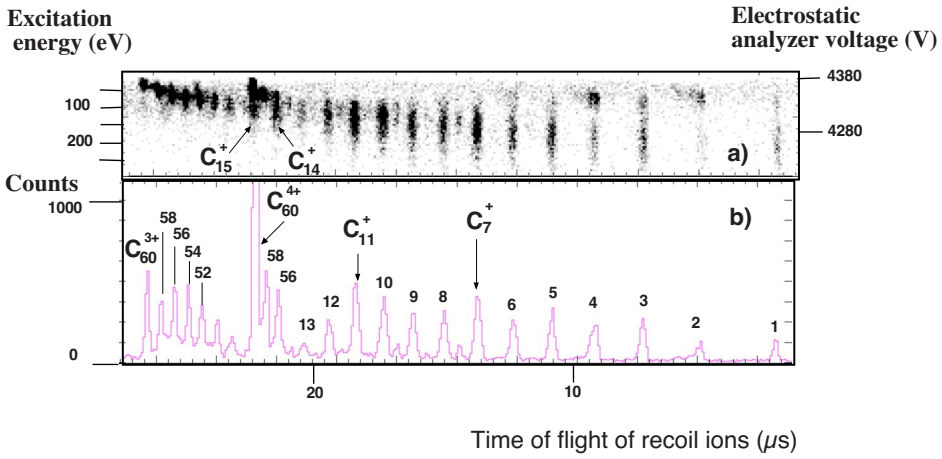

FIG. 5. (Color online) (a) EX-RI spectrum associated to the C_{60}^{4+*} intermediate parent ions recorded in collisions $F^{2+}+C_{60} \rightarrow F^{-}+C_{60}^{3+*}$ with an extra condition that one electron from TEI be detected. (b) Projection of (a) onto the horizontal axis. Evaporation, AF, and MF processes are observed. The large cross section for the production of C_{60}^{3+} leads to a weak peak in this spectrum due to the electrical noise on the PIPS detector.

with the well-established knowledge that the fast TEI is a near-threshold process. Hence, the internal energy of the intermediate C_{60}^{4+*} parent ions prior to the fragmentation can be estimated by the measured energy of the initial parent C_{60}^{3+*} minus the fourth ionization potential of $C_{60}(E_c - IP_4)$.

In contrary to the evaporation channels, a shift of about 10.4 eV obviously smaller than IP_4 is observed for the energy distributions of intact C_{60}^{4+} and C_{60}^{3+}. In the case of C_{60}^{4+} ions, the internal energy distribution is centered at 30.8 eV (=49.2 eV$-IP_4$). It is about 8 eV lower than that of the C_{60}^{3+} intact ions. Let us recall that in the case of C_{60}^{2+} prepared by H^+ impact, the internal energy was centered at 12 eV [18]. It is interesting to notice that due to the stability of C_{60}, the internal energy of intact C_{60} prepared in experiments varies in a large range and is centered around very different values from one case to another depending sensitively on the excitation dynamics. On the contrary, consistent with the cascade-statistical decay model, the first evaporation channels are opened in narrow energy windows with high-energy selectivity and are nearly independent of the parent charge.

C. Quadruply charged intermediate-parent ions: Asymmetrical fission

The triply charged fullerene peaks in the TOF spectrum [Fig. 5(b)] could result from several AF channels of the intermediate C_{60}^{4+} parent ions. For instance, at least two main channels $C_{60}^{4+} \rightarrow C_{56}^{3+}+C_4^+$ and $C_{60}^{4+} \rightarrow C_{56}^{3+}+C_2^+ + C_2$ can contribute to the peak C_{56}^{3+}. These two channels could be identified in a correlation spectrum between heavy and light fragments as shown in Fig. 6. They correspond respectively to the spots $C_{56}^{3+}+C_4^+$ and $C_{56}^{3+}+C_2^+$. The excitation energy distribution of the initial C_{60}^{3+*} parent ions was measured for each spot of this spectrum. The center of the distribution for all fission channels from the C_{60}^{4+*} intermediate ions is presented in Fig. 7 and Table I.

From Table I, one notices that the excitation energies for the AF channel $C_{60}^{4+} \rightarrow C_{58}^{3+}+C_2^+$ and the evaporation channel $C_{60}^{4+} \rightarrow C_{58}^{4+}+C_2$ (Table I) are very close. This result supports the two-step hypothesis on the fission process [23]. First, a C_2 fragment escapes from the fullerene cage and, second, one electron is captured by the multiply charged fullerene from the receding neutral dimer. The initial process involved in the two channels is similar and requires a very close amount of excitation energy. Figure 7 shows also that the excitation energy for the channel $C_{60}^{4+} \rightarrow C_{56}^{3+}+C_4^+$ is about 5.1 eV larger than for the channels involving the emission of a dimer, $C_{60}^{4+} \rightarrow C_{58}^{3+}+C_2^+$ and $C_{60}^{4+} \rightarrow C_{58}^{4+}+C_2$. It is explained by the fact that a larger number of bonds have to be broken for extracting a C_4^+ than a C_2^+. However, the excitation energies for the channels $C_{60}^{4+} \rightarrow C_{56}^{3+}+C_4^+$ and $C_{60}^{4+} \rightarrow C_{56}^{3+}+C_2^+ + C_2$ are measured to be very close. This is consistent with the assumption that the emission of the two fragments C_2^+ and C_2 is a sequential process [24] instead of a two-step process, i.e., asymmetrical fission $C_{60}^{4+} \rightarrow C_{56}^{3+} + C_4^+$ followed by dissociation of the small fragment C_4^+. The last scenario would need an extra amount of energy for the second step $C_4^+ \rightarrow C_2^+ + C_2$.

The data of AF in the Table I concerning the C_{60}^{4+*} intermediate-parent-ions are displayed in Fig. 8 according to

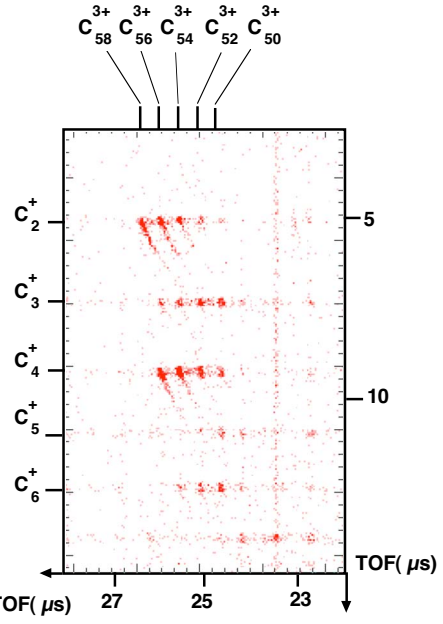

FIG. 6. (Color online) Correlation spectrum of recoil fragments. The TOF of the heavy and light fragments from AF of C_{60}^{4+*} intermediate parent ions are plotted, respectively, along the horizontal and vertical axes.

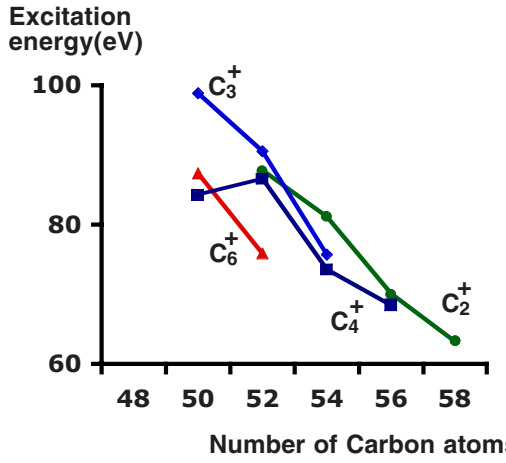

FIG. 7. (Color online) Center E_c of the excitation energy distributions for AF channels from C_{60}^{4+*} intermediate parent ions. The values are given for all fission channels observed in Fig. 6.

the number of ejected light fragments. For the reactions $C_{60}^{4+} \rightarrow C_{60-2m-n}^{3+} + C_n^+ + mC_2$, with $n=2,4,6$, the number of light fragments is given by $1+m$. In the case of the reactions $C_{60}^{4+} \rightarrow C_{60-2m-4}^{3+} + C_3^+ + C + mC_2$, the number of emitted light fragments is $2+m$ due to the ejection of a carbon atom to maintain stable the structure of the fullerene cage [24]. The main tendency shown in Fig. 8 is that the excitation energy increases with the number of ejected light fragments.

D. C_{60}^{4+} and C_{60}^{5+} intermediate parent ions: Multifragmentation

To study the MF process of the C_{60}^{4+} intermediate parent ions, we recorded an EX-RI spectrum (not shown here) for events in which one electron and at least two charged fragments were detected. The excitation energy distribution of the initial parent ions C_{60}^{3+*} was obtained by partial projections of each spot onto the vertical axis. For channels leading to monocharged fragments C_n^+ $(1 \leqslant n \leqslant 15)$ and to C_{15}^{2+}, C_{19}^{2+}, and C_{23}^{2+} doubly charged fragments, the results are presented in Fig. 9 and Tables IV and V. The energy distributions corresponding to lighter fragments were rather well reproduced with a Gaussian distribution. However, for fragments of medium size (C_{15}^+-C_9^+), a better agreement was found using a log-normal distribution with a small asymmetry of about 0.8. Details will be given in a forthcoming paper. With a similar method, we studied the MF of intermediate parent ions C_{60}^{5+} resulting from the fast double TEI of the initial parent ions C_{60}^{3+*}. An EX-RI spectrum was built for events in which two electrons and at least two charged fragments were detected (Fig. 10). The center and width of the excitation energy distribution associated with each fragment are also given in Fig. 9 and Tables IV and V.

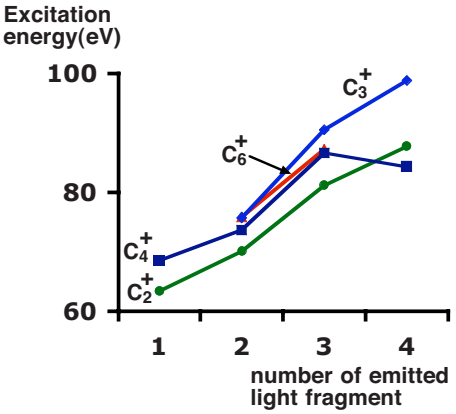

FIG. 8. (Color online) Same as Fig. 7, but the excitation energy values are given versus the number of emitted light charged fragments.

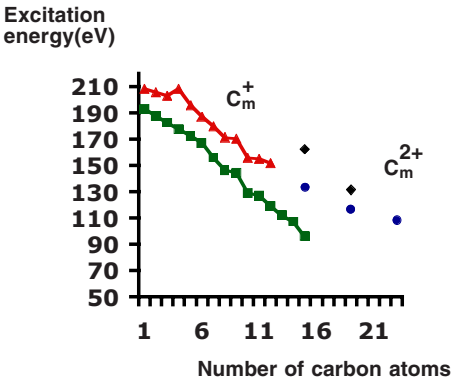

FIG. 9. (Color online) Center of the excitation energy distributions of initial parents C_{60}^{3+} for MF processes related to the detection of a light fragment C_n^+ $(n=1-15)$ from C_{60}^{4+} (squares) and C_{60}^{5+} (triangles) intermediate parent ions. Values related to the detection of C_n^{2+} $(n=15,19,23)$ from C_{60}^{4+} (circles) and C_{60}^{5+} (diamonds) intermediate parent ions.

An increase of the excitation energy with decreasing size of the fragment is observed clearly in Fig. 9. In the case of C_{60}^{4+} parent ions, the excitation energy decreases quasilinearly from 193 eV to 96 eV for producing monocharged fragments C_n^+ with n from 1 to 15. For C_{60}^{5+} parent ions, the excitation energy decreases from 210 eV to 152 eV for producing fragments C_n^+ with n from 1 to 12. The difference in

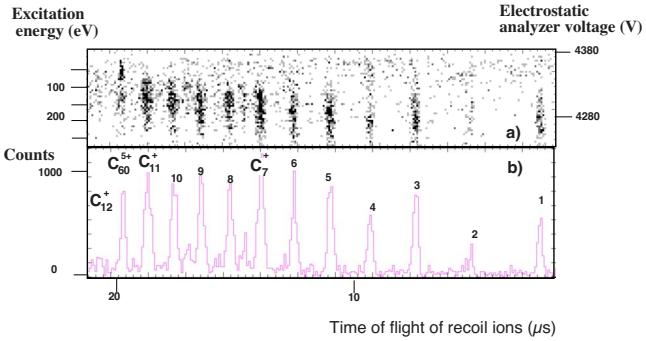

FIG. 10. (Color online) (a) EX-RI spectrum associated to the intermediate parent ions C_{60}^{5+} recorded in collisions $F^{2+}+C_{60} \rightarrow F^- + C_{60}^{3+*}$ with an extra condition that two electrons from TEI be detected. (b) Projection from (a) onto the horizontal axis. MF process is observed for C_{60}^{5+}.

TABLE IV. E_c: center of the measured excitation energy distributions of the initial parent ions C_{60}^{3+} undergoing first the fast TEI and then the MF from the intermediate parent ions C_{60}^{4+} or C_{60}^{5+}. Values are given in eV.

	Multifragmentation of intermediate parent ions C_{60}^{4+}		Multifragmentation of intermediate parent ions C_{60}^{5+}	
Number of C atoms in the detected fragment C_n^+ or C_n^{2+}	Emission of C_n^+	Emission of C_n^{2+}	Emission of C_n^+	Emission of C_n^{2+}
1	193		208	
2	188		205	
3	182		203	
4	177		208	
5	172		196	
6	167		187	
7	156		180	
8	146		171	
9	144		170	
10	129		156	
11	127		155	
12	119		152	
13	112			
14	107			
15	96	134		162
19		117		131
23		108		

measured excitation energy for producing a monocharged fragment of a given size from the C_{60}^{4+*} and C_{60}^{5+*} intermediate parent ions is almost constant. For instance, it is measured to be 25 eV for C_{11}^+ and 20 eV for C_3^+. The mean value corresponds roughly to the fifth IP of the C_{60} IP_5 =21.4 eV estimated by linear extrapolation of the data in Ref. [19]. This indicates that a fragment of a given size is produced at roughly the same internal energy whatever the charge of the parent ion. Therefore, the MF process seems to be quite sensitive to the internal energy rather than to the charge of the C_{60}^{r+} in the present narrow charge range (r =4,5).

Figure 11 gives the MF profiles of C_{60}^{4+} including monocharged fragments (C_n^+, n=1–15) versus the measured excitation energy of initial C_{60}^{3+*} parents. A shift to smaller fragments is noticed with increasing energy. From this figure or using the data of the Tables IV and V and the relation E_c-Δ-IP_4, we estimated the appearance energy of a C_n^+ fragment from the intermediate C_{60}^{4+} parent ions via MF. The obtained values vary in a large range from 120 eV for producing C^+ to 40 eV for C_{15}^+. These values are very different from the results obtained in collisions between C_{60}^+ and atomic targets (see Fig. 3 of Ref. [25]). In Ref. [25], the appearance energy for producing C_n^+ ($3 \leqslant n \leqslant 15$) from the C_{60}^+ parent ions was measured to be nearly independent of the mass of the fragments at around 80 eV. This energy at which small fragments first appear was considered as marking the onset of a "phase transition" in the hot C_{60} [25]. The energy range corresponding to the evolution of fragment mass distribution from that containing only fullerenes to the one with only small fragments was found to be from 80 to 225 eV for C_{60}^+. It corresponds to a large energy window in which the AF and MF compete. In our case for quadruply charged C_{60}^{4+}, the lower limit in energy for the MF was found to be 40 eV, corresponding to the appearance energy of C_{15}^+. On the other hand, the highest internal energy for producing fullerene fragments, estimated using the values in Tables IV and V with the relation $E_c+\Delta-IP_4$, was found at 98 eV for the case of C_{50}^{3+}-C_3^+ (Fig. 6). The energy window in which the AF and MF compete is therefore in a range from 40 to 98 eV in the present case. This energy window is narrower and centered at a lower value comparing to the results of singly charged C_{60}. This divergence is obviously related to the charge effect. Indeed, at the same internal energy, a multicharged C_{60} is less stable than a monocharged one. Due to the additional repulsive force, more fragmentation channels are available. It has been already demonstrated by a large number of experiments that in the low-energy range, C_{60}^+ ions decay only by successive emission of C_2 units, while multicharged C_{60} ions can lose other even- or odd-numbered fragments C_n^+ (n=1–8) [8,24,26–28]. The present experiment provides clear evidence that at lower internal energy the MF channels are also opened for highly charged C_{60}^{4+} ions. Our measurement suggests that a charge-effect-assisted "phase change" of C_{60}^{4+} occurs at 40 eV.

TABLE V. Δ: width (FWHM) of the measured excitation energy distributions of the initial parent ions C_{60}^{3+} (as in Table II) undergoing first the fast TEI and then the MF from the intermediate parent ions C_{60}^{4+} and C_{60}^{5+}. Values are given in eV.

	Multifragmentation of intermediate parent ions C_{60}^{4+}	
Number of C atoms in the detected fragment C_n^+ or C_n^{2+}	Emission of C_n^+	Emission of C_n^{2+}
1	53.8	
2	53.8	
3	53.8	
4	53.8	
5	53.8	
6	53.8	
7	53.8	
8	58.7	
9	51.9	
10	45.5	
11	45.1	
12	47.8	
13	39.7	
14	42.0	
15	35	30
19		41.3
23		36.6

E. Sequential process in multifragmentation

As shown in Fig. 9, the excitation energy of the parent ions that emit C_n^{2+} ($n=15,19,23$) via MF was found surprisingly high compared to events where only monocharged medium-sized fragments, such as, for instance, C_{15}^+, were involved. This detailed information provides some insight into the dynamics of MF. If the MF were a spontaneous process and the charge of each fragment were to result from a homogeneous spatial distribution of the total charge followed by a random fissure of the C_{60} cage, one would expect equal excitation energy for the above two types of channels involving fragments of the same size—for example, C_{15}^+ and C_{15}^{2+}. A tentative explanation for the observed important difference in energy is proposed here. It has already been observed in a previous study that the emission of a doubly charged fragment of medium size occurred for C_{60} at highly charged state via the AF [29]. The measured very low branching ratios of these channels compared to that of emission of singly charged fragment were interpreted as due to the relatively high fission barriers. Therefore the emission of a C_n^{2+} occurred mainly at higher excitation energies. Keeping this in mind, we interpret the MF with the emission of a C_n^{2+} as a sequential multistep process. It includes first the fission of the C_{60}^{r+} (4+ or 5+) leading to the ejection of a C_n^{2+} and then the breakdown of the residual hot fullerene. A similar multistep process has been already suggested in fast heavy-ion C_{60} collisions [30]. By measuring the kinetic energy release (KER) of small fragments, Majima *et al.* differentiated the direct MF at larger KER value from the sequential fragmentation at smaller KER value. The last process corresponds to the production of a smaller fragment from an intermediate larger fragment. Our result, consistent with the description of Ref. [30], supports the hypothesis that the MF of multiply charged C_{60} ions might occur in a sequential multistep process.

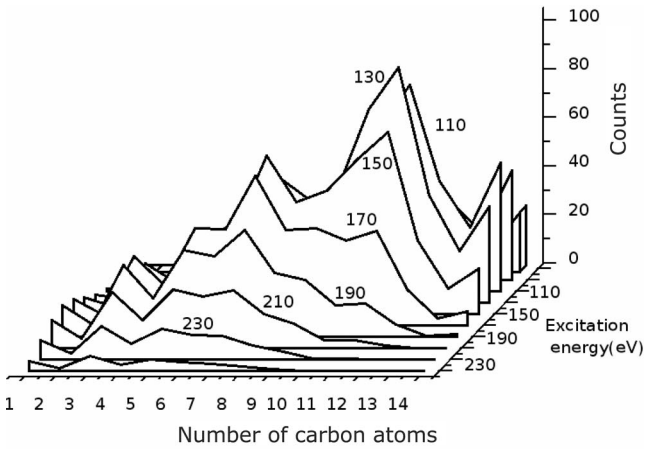

FIG. 11. Mass distribution associated to different excitation energies from 70 eV to 230 eV for the MF channels from the C_{60}^{4+} intermediate parent ions.

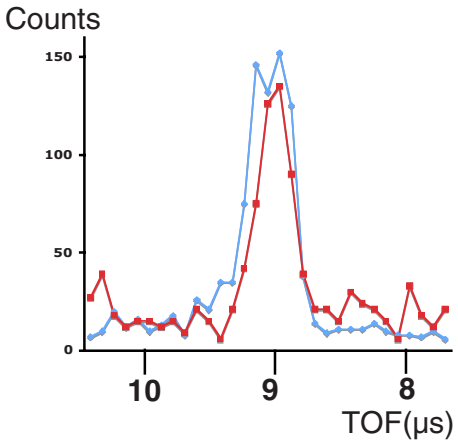

FIG. 12. (Color online) Comparison between the TOF peaks of C_4^+ due to the AF (circles) and due to the MF processes (squares) from C_{60}^{4+} intermediate parent ions.

In Fig. 12, we compare the profile of the TOF peaks of C_4^+ due to the AF ($C_{60}^{4+} \rightarrow C_{56}^{3+} + C_4^+$) and due to the MF processes from C_{60}^{4+} intermediate parent ions. The peak due to the AF is observed broader than that from the MF. This is another indication that the C_4^+ fragment of MF comes from a sequential multistep process. The C_4^+ fragments due to MF may result from an intermediate fragment of lower charge state leading to weaker Coulomb repulsion and, therefore, to a smaller initial kinetic energy spread and, then, a narrower width in the TOF spectrum.

IV. CONCLUSION

We have applied the CIDEC method to measure the internal excitation energy of multicharged C_{60}^{r+} $(r=3,4,5)$ prepared in the primary three-electron capture process $F^{2+}+C_{60}\rightarrow F^{-}+C_{60}^{3+*}$ for a large number of fragmentation channels. The internal energy distribution of C_{60}^{3+} for the evaporation channels, $C_{60}^{3+}\rightarrow C_{60-2m}^{3+}+mC_2$, has been simulated using a cascade statistical evaporation model. The dissociation energies D^{3+} of triply charged fullerenes have been derived and compared to theoretical values. The fast TEI leading to the intermediate parent ions C_{60}^{4+} has been demonstrated to be a near-threshold process in the case studied by comparing the excitation energy profile for the evaporation channels from C_{60}^{3+} and C_{60}^{4+}. The center and width of all detected AF channels from C_{60}^{4+} and MF channels from C_{60}^{4+} and C_{60}^{5+} intermediate parent ions have been presented. Although the internal energy of the intermediate parent ions associated with a given small fragment from MF seems to be independent of the charge in the range $r=4,5$, the internal energy window in which the AF and MF compete was found much lower and narrower for the C_{60}^{4+} (40–100 eV) than in the case of C_{60}^{+} (80–220 eV). This phenomenon is considered as a charge-effect-assisted "phase change" of C_{60} that occurs at a much lower energy (40 eV) than in the case of C_{60}^{+} (80 eV). A sequential multistep process is proposed for the MF of multicharged C_{60} based on the analysis of the internal energy for channels with the ejection of a doubly charged small fragment and on the comparison of the TOF peak profiles of a singly charged fragment resulting from AF and MF.

ACKNOWLEDGMENTS

The authors are grateful for fruitful and stimulating discussions with C. Bordas, B. Concina, F. Lépine, M-A. Lebeault, and F.Calvo.

[1] I. V. Hertel *et al.*, in *Advances in Atomic, Molecular, and Optical Physics*, edited by B. Bederson and H. Walther (Elsevier Academic Press Inc., San Diego, 2005), Vol. 50, pp. 219–286.
[2] P. N. Juranic *et al.*, Phys. Rev. A **73**, 042701 (2006).
[3] A. Reinköster *et al.*, J. Phys. B **37**, 2135 (2004).
[4] V. Foltin *et al.*, Chem. Phys. Lett. **289**, 181 (1998).
[5] P. Scheier *et al.*, Int. J. Mass Spectrom. Ion Process. **138**, 77 (1994).
[6] D. Hathiramani, K. Aichele, W. Arnold, K. Huber, E. Salzborn, and P. Scheier, Phys. Rev. Lett. **85**, 3604 (2000).
[7] R. Ehlich *et al.*, J. Chem. Phys. **104**, 1900 (1996).
[8] S. Martin, L. Chen, R. Brédy, J. Bernard, M. C. Buchet-Poulizac, A. Allouche, and J. Desesquelles, Phys. Rev. A **66**, 063201 (2002).
[9] L. Chen, B. Wei J. Bernard, R. Brédy, and S. Martin, Phys. Rev. A **71**, 043201 (2005).
[10] J. Opitz *et al.*, Phys. Rev. A **62**, 022705 (2000).
[11] S. Tomita, J. U. Andersen, C. Gottrup, P. Hvelplund, and U. V. Perdersen, Phys. Rev. Lett. **87**, 073401 (2001).
[12] A. Rentenier *et al.*, J. Phys. B **37**, 2429 (2004).
[13] J. Appell, *Collision Spectroscopy* (Cooks Plenum Press, New York, 1978), p. 227.
[14] T. Andersen, Phys. Lett. **394**, 157 (2004).
[15] P. G. Fournier, J. Fournier, F. Salama, D. Stark, S. D. Peyerimhoff, and J. H. D. Eland, Phys. Rev. A **34**, 1657 (1986).
[16] O. Furuhashi *et al.*, Chem. Phys. Lett. **337**, 97 (2001).
[17] S. Martin *et al.*, Europhys. Lett. **74**, 985 (2006).
[18] L. Chen, S. Martin, J. Bernard, and R. Brédy, Phys. Rev. Lett. **98**, 193401 (2007).
[19] G. Seifert *et al.*, Phys. Lett. A **211**, 357 (1996).
[20] J. U. Andersen *et al.*, J. Chem. Phys. **114**, 6518 (2001).
[21] B. Concina *et al.*, Eur. Phys. J. D **34**, 191 (2005).
[22] S. Diaz-Tendero *et al.*, J. Chem. Phys. **119**, 5545 (2003); P. Diaz-Tendero, Ph.D. thesis, Autonomous University of Madrid, 2005.
[23] P. Scheier, B. Dunser, and T. D. Mark, Phys. Rev. Lett. **74**, 3368 (1995).
[24] L. Chen, J. Bernard, A. Denis, S. Martin, and J. Desesquelles, Phys. Rev. A **59**, 2827 (1999).
[25] E. E. B. Campbell *et al.*, Chem. Phys. Lett. **253**, 261 (1996).
[26] A. Reinköster *et al.*, Europhys. Lett. **43**, 653 (1998).
[27] S. Martin, L. Chen, J. Bernard, M. C. Buchet-Poulizac, B. Wei, and R. Brédy, Phys. Rev. A **73**, 013204 (2006).
[28] R. Vandenbosch, B. P. Henry, C. Cooper, M. L. Gardel, J. F. Liang, and D. I. Will, Phys. Rev. Lett. **81**, 1821 (1998).
[29] L. Chen *et al.*, Europhys. Lett. **58**, 375 (2002).
[30] T. Majima *et al.*, Phys. Scr. **T92**, 179 (2001).